Chinese Journal of Chemical Engineering 26 (2018) 207–212

Contents lists available at ScienceDirect

Chinese Journal of Chemical Engineering

journal homepage: www.elsevier.com/locate/CJChE

Article

Bi-/multi-modal pore formation of PLGA/hydroxyapatite composite scaffolds by heterogeneous nucleation in supercritical CO_2 foaming☆

Xin Xin, Yixin Guan *, Shanjing Yao

College of Chemical and Biological Engineering, Zhejiang University, Hangzhou 310027, China

ARTICLE INFO

Article history:
Received 10 February 2017
Received in revised form 27 March 2017
Accepted 7 April 2017
Available online 22 April 2017

Keywords:
Supercritical carbon dioxide
Foam
Tissue engineering
PLGA scaffolds
Hydroxyapatite
Bi-/multi-modal pore

ABSTRACT

Scaffolds with multimodal pore structure are essential to cells differentiation and proliferation in bone tissue engineering. Bi-/multi-modal porous PLGA/hydroxyapatite composite scaffolds were prepared by supercritical CO_2 foaming in which hydroxyapatite acted as heterogeneous nucleation agent. Bimodal porous scaffolds were prepared under certain conditions, *i.e.* hydroxyapatite addition of 5%, depressurization rate of 0.3 MPa·min^{-1}, soaking temperature of 55 °C, and pressure of 9 MPa. And scaffolds presented specific structure of small pores (122 μm ± 66 μm) in the cellular walls of large pores (552 μm ± 127 μm). Furthermore, multimodal porous PLGA scaffolds with micro-pores (37 μm ± 11 μm) were obtained at low soaking pressure of 7.5 MPa. The interconnected porosity of scaffolds ranged from (52.53 ± 2.69)% to (83.08 ± 2.42)% by adjusting depressurization rate, while compression modulus satisfied the requirement of bone tissue engineering. Solvent-free CO_2 foaming method is promising to fabricate bi-/multi-modal porous scaffolds in one step, and bioactive particles for osteogenesis could serve as nucleation agents.

1. Introduction

Bone tissue engineering (bTE) has been a hot research field to regenerate osseous tissue [1,2]. For osteogenesis, there are two basic development pathways, *i.e.* direct ossification and endochondral ossification [3]. Small pores ranging in the order of 100 μm favor hypoxic conditions and induce osteochondral formation before osteogenesis, while large pores with the pore size of >300 μm can lead to direct osteogenesis *via* a process analogous to intramembranous ossification [4]. Furthermore, the presence of micro-pores, with pore size ranging from 1 to 50 μm, may promote the transport of nutrient and metabolic waste in the interior of the pore structure [5]. Hence, fabrication of scaffolds with bi-/multi-modal pores is very important and imperative.

There are two typical methods to fabricate bi-/multi-modal porous scaffolds, *i.e.* solvent casting/particle leaching and supercritical CO_2 ($scCO_2$) foaming. Between them, solvent casting/particle leaching is one of the most popular and traditional methods to prepare scaffolds, in which salt particles are used as porogen [6]. And scaffolds can be obtained easily by evaporating solvent and washing out of porogen. This method, however, is limited in tissue engineering to some extent due to the use of organic solvents. Under this situation, $scCO_2$ foaming has its own advantages in preparing tissue engineering scaffolds without the use of organic solvents and high temperature [7]. Mooney *et al.* [8] firstly applied $scCO_2$ foaming to prepare tissue engineering scaffolds in 1990s. Bimodal porous scaffolds were successfully prepared by $scCO_2$ foaming when combining with particle leaching [9,10]. Also an interesting phenomenon was observed that particles might serve to facilitate heterogeneous nucleation in $scCO_2$ foaming process, although NaCl was not an ideal nucleation agent [11,12].

The process of $scCO_2$ foaming consists of three main aspects: dissolution of CO_2 into polymer, nucleation at the moment of depressurization, and the growth of pores [8]. According to classical nucleation theory, both of heterogeneous and homogeneous nucleation were emerging in the course of nucleation when the third phase existed [13,14]. In general, the activation energy for heterogeneous nucleation, which is relevant with interfacial tension of the third phase in foaming system, is much lower than that of homogeneous nucleation. Namely, gas nuclei formed by heterogeneous nucleation emerged earlier than those formed by homogeneous nucleation [15]. Then CO_2 diffused into gas nuclei to form pores. Therefore, gas nuclei formed by heterogeneous nucleation had a longer period to grow large pores. Most importantly, these earlier small pores facilitated the coalescence of neighboring pores to form large pores, while the pores rupture could lead to micro-pores within the pore walls [16]. Thus, bi-/multi-modal porous scaffolds can be fabricated by simple $scCO_2$ foaming if an efficient nucleation agent is used.

Ceramics, a kind of bioactive substances, is often used as an additive to fabricate tissue engineering scaffolds in the process of $scCO_2$ foaming. It was reported that hydroxyapatite (HA) and β-tricalcium phosphate (β-TCP) could also act as heterogeneous nucleation agent in the foaming process [17–19]. As we know, bioactive HA or β-TCP are natural components of bone, which can interact with the surrounding bone

☆ Support by the National Natural Science Foundation of China (21276225, 21476196).
* Corresponding author.
E-mail address: guanyx@zju.edu.cn (Y. Guan).

http://dx.doi.org/10.1016/j.cjche.2017.04.005
1004-9541/

[20,21]. PLGA scaffolds with HA or β-TCP as filler were biocompatible and osteoconductive in bone cell culture [22]. Hence, the addition of HA or β-TCP particles served as the third phase in $scCO_2$ foaming not only facilitate the fabrication of bi-/multi-modal porous scaffolds, but also can guide cells growth subsequently [17]. In this paper, bi-/multi-modal porous PLGA/HA composite scaffolds will be fabricated by simple $scCO_2$ foaming, in which HA particles are used as the third phase to reinforce the process of heterogeneous nucleation. PLGA scaffolds obtained are biocompatible and osteoconductive due to the addition of HA. The effects of HA addition amount, soaking temperature, pressure, and depressurization rate on the structure of scaffolds will be studied in detail. Specially, bi-/multi-modal pore formation is discussed considering the nucleation theory. This novel solvent-free $scCO_2$ foaming method has great potential in fabricating bi-/multi-modal bone tissue engineering scaffolds incorporated by bioactive substances under mild conditions.

2. Materials and Methods

2.1. Materials

PLGA (lactide:glycolide = 85:15, M_w = 140 kDa, polydispersity index (PDI) = 1.73) in a granular form was purchased from Shenzhen Esun Industrial Co., Ltd. (Shenzhen, China). Hydroxyapatite (HA) was purchased from Shanghai Rebone Biomaterials Co., Ltd. (Shanghai, China). Carbon dioxide (99.9% purity) was supplied by Hangzhou Jingong Gas Co. Ltd. (Zhejiang, China). All other chemicals were of reagent grade and utilized without further purification.

2.2. Preparation of PLGA samples

Firstly, PLGA microspheres were produced by emulsion-solvent evaporation [12]. Concretely, PLGA granules were dissolved in dichloromethane to obtain 10% ($g \cdot ml^{-1}$, w/v) PLGA solution, which was then mixed with 1% polyvinyl alcohol (PVA) aqueous solution and processed by shearing. After evaporation of dichloromethane, PLGA microspheres were collected by centrifugation and freeze-drying. Secondly, hydroxyapatite particles used as heterogeneous nucleation agent were mixed with PLGA microspheres in a certain proportion by a glass bead breaker (MM200, Retsh, Germany). Finally, the physical mixtures of PLGA microspheres and HA particles were mold-pressed at 10 MPa in a die for 1 min to get cylindrical flakes. The thickness of the samples was limited to 2 mm with a diameter of 13 mm by 0.3 g.

2.3. The $scCO_2$ foaming process

Supercritical system (SFE-500MR-2-FMC 10, Thar, USA) was applied in the foaming process, which was mainly consisted of an autoclave of 100 ml [12]. In this experiment, PLGA flakes with different HA fractions were placed in the autoclave and equilibrated for 2 h. Temperature fluctuation was controlled to be ±1 °C and pressure fluctuation ±1 MPa. After $scCO_2$ foaming, the porous scaffolds could be removed from the autoclave and stored in a desiccator for further analysis.

2.4. Characterization of porous PLGA scaffolds

The pore morphologies of porous scaffolds were firstly observed by scanning electron microscopy (SEM) (SU8010, Hitachi, Japan). The scaffolds were freeze-fractured in liquid nitrogen, sputter-coated with platinum. The pore sizes of PLGA scaffolds were then analyzed by image processing analysis software (Image Pro Plus 6.0, Media Cybernetics, USA) after obtaining SEM images.

The interconnected porosities of scaffolds were obtained using mercury intrusion porosimetry (AutoPore IV 9500 V1.07, Micromeritics, USA). The total porosities of scaffolds could be calculated from the density of PLGA before and after foaming, by Eq. (1):

$$\varphi = 1 - \rho_2/\rho_1 \quad (1)$$

where ρ_1 and ρ_2 were the density of PLGA before and after foaming respectively [23].

The static compression properties of scaffolds were measured using a material testing machine (Zwick/Roell Z2.5, Zwick/Roell, Germany). The compression modulus (E) was the slope of the initial linear part by depicting the curve of stress *versus* strain. All compression experiments were performed in triplicates and the averages were used.

3. Results and Discussion

3.1. The operating parameters of $scCO_2$ foaming

Prior to $scCO_2$ foaming, the morphologies of PLGA microspheres obtained and HA raw particles were observed and the SEM images are shown in Fig. 1. The diameter of spherical PLGA micro-particles was in the order of 10 μm, and the size of HA particles was similar to that of PLGA microparticles. In this case, it was relatively easy to achieve uniform mixing for PLGA matrix and HA particles.

For $scCO_2$ foaming process, soaking temperature and pressure had a significant effect on CO_2 solubility and diffusivity in PLGA matrix. At the moment of depressurization, the number of gas nuclei mainly depended on the degree of CO_2 supersaturation, *i.e.* the depressurization rate of foaming system. Specifically, the HA amount acting as a nucleation agent could have a profound effect on the pore structure of scaffolds. Hence, it was necessary to discuss the effects of the HA addition amount, soaking temperature, pressure and depressurization rate on the pore structure of scaffolds in order to fabricate bi-/multi-modal porous PLGA scaffolds with ideal properties. The operating parameters of $scCO_2$ foaming are listed in Table 1.

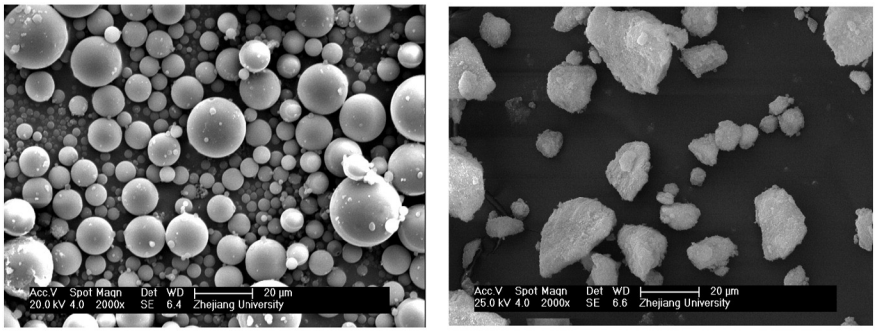

Fig. 1. SEM images of PLGA microspheres obtained and HA raw particles. (a) PLGA microparticles; (b) HA particles.

Table 1
Summary of operating parameters of $scCO_2$ foaming

No.	HA amount/%	Temperature/°C	Pressure/MPa	Depressurization rate/MPa·min^{-1}
Effect of HA addition amount				
1	5	55	9	1.5
2	10	55	9	1.5
3	20	55	9	1.5
Effect of soaking temperature				
4	5	35	9	4.5–6
5	5	45	9	4.5–6
6	5	55	9	4.5–6
Effect of soaking pressure				
7	5	35	7.5	4.5–6
8	5	35	9	4.5–6
9	5	35	12	4.5–6
10	5	35	15	4.5–6
Effect of depressurization rate				
11	5	55	9	3–6
12	5	55	9	1.5
13	5	55	9	0.3
14	5	55	9	0.1

3.2. HA particles as the heterogeneous nucleation agent in $scCO_2$ foaming

HA is a bioactive substance and can also act as a heterogeneous nucleation agent in $scCO_2$ foaming [21,22]. As we know, gas nuclei formed by both heterogeneous and homogeneous nucleation grew to pores. With the addition of HA as the third phase, gas nuclei formed by heterogeneous nucleation increased accordingly. Namely, those early pores due to heterogeneous nucleation merged with neighboring pores to form large pore, while pore rupture led to small pores or even micro-pores within the large pore walls. Finally, bi-/multi-modal porous scaffolds could be fabricated.

The effect of HA addition on pore structure should be well investigated to fabricate bi-/multi-modal PLGA scaffolds. SEM images and pore size at different amounts of HA are shown in Figs. 2 and 3(a) respectively, and bimodal porous scaffolds were successfully prepared, in which small pores were in the walls of large pores. With the increase of HA from 5% to 20%, the size of large pores decreased from (995 ± 226) μm to (409 ± 102) μm, and the size of small pores also decreased from (104 ± 66) μm to (62 ± 29) μm. Besides, the thickness of pore wall firstly increased from (15 ± 4) μm to (53 ± 22) μm, and then decreased to (29 ± 8) μm. According to the classical nucleation theory, two competitions existed at the same time during foaming process [13,14,24,25]. The first one was the competition between gas diffusing to form gas nuclei and gas diffusing into nucleated pores. And the second one was between gas diffusing out of the skin and gas diffusing into nucleated pores [17]. With the increase of HA addition amount in flakes, the nucleation sites provided by HA particles increased to strengthen the heterogeneous nucleation, which could restrain the diffusivity of CO_2 into nucleated pores to form larger pores to some extent given CO_2 solubility kept constant. Therefore with the increase of HA addition amount from 5% to 20%, the size of large pores and small pores both decreased, while the number of pores increased [17,26,27]. Moreover, HA addition amount had an effect on the thickness of pore wall, which is relevant with mechanical property of scaffolds.

3.3. Fabrication of bi-/multi-modal PLGA porous scaffolds by $scCO_2$ foaming

3.3.1. The effect of soaking temperature on the pore structure of scaffolds

As shown in Figs. 3(b) and 4, bimodal porous PLGA scaffolds were well prepared by $scCO_2$ foaming at 5% HA addition amount, soaking pressure of 9 MPa, depressurization rate of 4.5–6 MPa·min^{-1} with different soaking temperatures. With the soaking temperature increase from 35 °C to 45 °C, the size of large pores decreased from (456 ± 182) μm to (370 ± 111) μm, and then increased to (611 ± 223) μm at 55 °C. In the whole process, the size of small pores increased from (64 ± 24) μm to (112 ± 29) μm, and the pore walls were relatively thin with several micrometers.

The CO_2 solubility decreases with the increase of soaking temperature, while the diffusivity of CO_2 in PLGA is enhanced [26,28]. Even though there are less CO_2 dissolved in PLGA available for nucleation and pore growth at higher temperature, the growth rate of pores increases due to the increased CO_2 diffusivity and less gas nuclei. So scaffolds with large pores could be easily prepared at high temperature, for example 55 °C. According to this work, bone tissue engineering scaffolds with bimodal porous structure could be successfully fabricated at a near ambient temperature of 35 °C. The low temperature makes $scCO_2$ foaming an ideal method to incorporate thermal sensitive bioactive substances into scaffolds such as protein as bone growth factor.

3.3.2. The effect of soaking pressure on the pore structure of scaffolds

As shown in Figs. 3(c) and 5, it is very inspiring that multimodal porous, bimodal microporous, and cellular scaffolds were all obtained by altering the soaking pressure. With the increase of soaking pressure from 7.5 MPa to 9 MPa, multimodal porous scaffolds were successfully prepared. And the size of large pores increased from (385 ± 149) μm to (458 ± 177) μm, while the size of small pores and micro-pores kept nearly constant. Continually, when the pressure increased to 12 MPa, bimodal microporous scaffolds were fabricated. And the size of small pores was (148 ± 39) μm, while the size of micro-pores was (20 ± 5) μm. Cellular scaffolds only with micro-pores were obtained when the pressure increased further to 15 MPa.

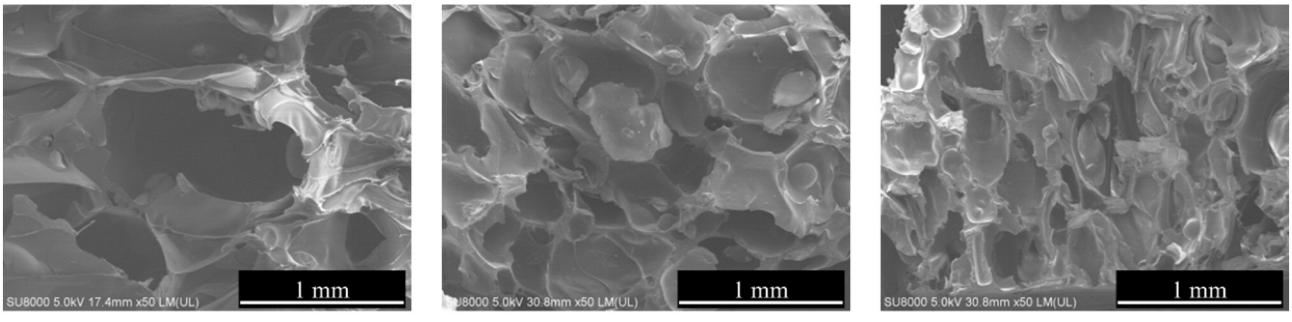

Fig. 2. The effects of addition of HA as a heterogeneous nucleation agent on the pore structure of PLGA scaffolds. (a) HA amount of 5%; (b) HA amount of 10%; (c) HA amount of 20% (temperature of 55 °C, pressure of 9 MPa, depressurization rate of 1.5 MPa·min^{-1}).

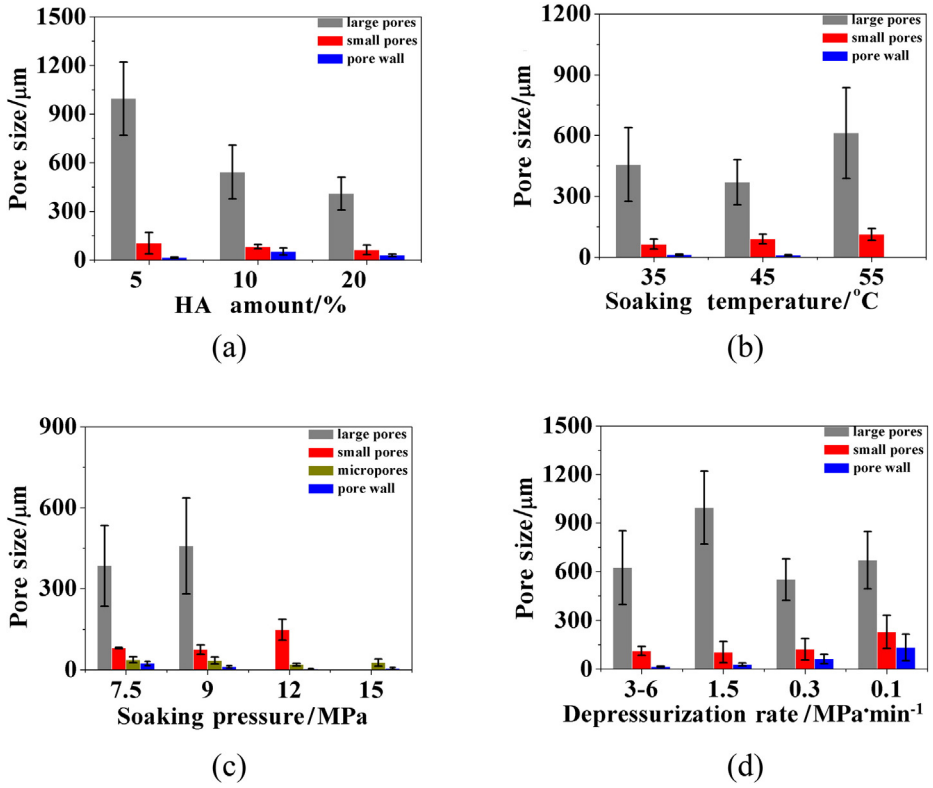

Fig. 3. The pore size of scaffolds fabricated at different $scCO_2$ foaming process. (a) Effect of HA amount (run 1–3); (b) effect of soaking temperature (run 4–6); (c) effect of soaking pressure (run 7–10); (d) effect of depressurization rate (run 11–14).

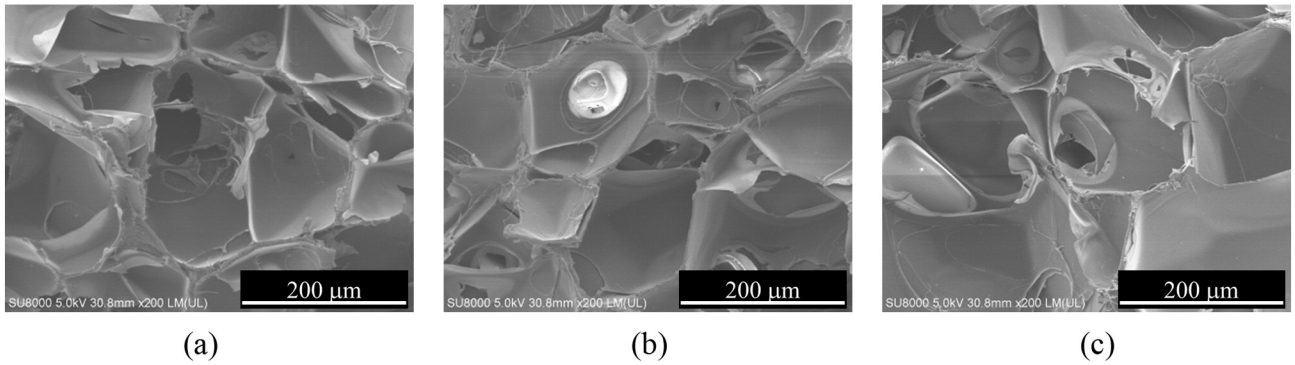

Fig. 4. The effects of soaking temperature on the pore structure of PLGA scaffolds. (a) Temperature of 35 °C; (b) temperature of 45 °C; (c) temperature of 55 °C (HA amount of 5%, soaking pressure of 9 MPa, depressurization rate of 4.5–6 MPa·min^{-1}).

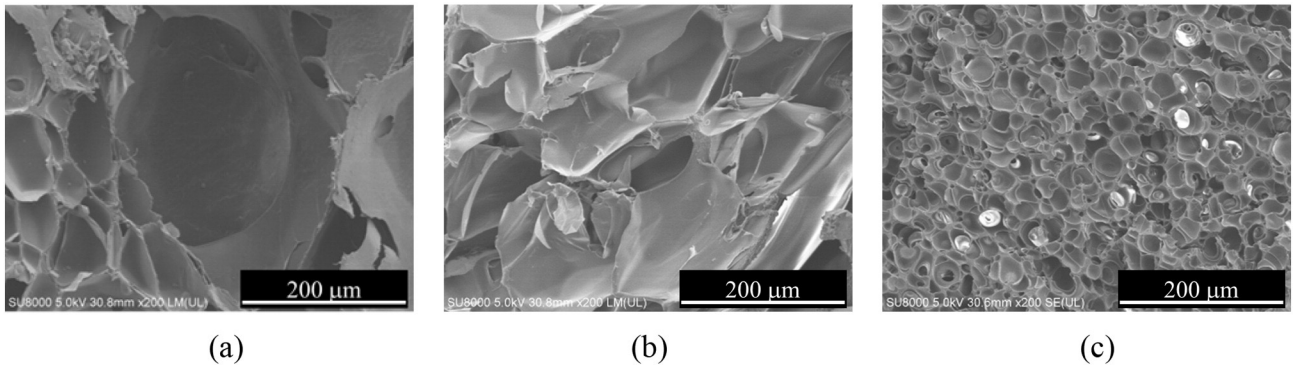

Fig. 5. The effects of soaking pressure on the pore structure of PLGA scaffolds. (a) Pressure of 7.5 MPa; (b) pressure of 12 MPa; (c) pressure of 15 MPa (HA amount of 5%, soaking temperature of 35 °C, depressurization rate of 4.5–6 MPa·min^{-1}).

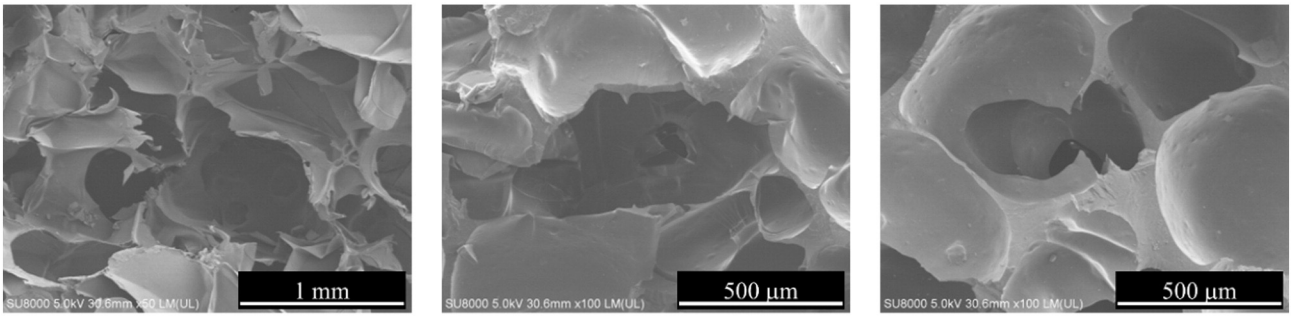

Fig. 6. The effects of depressurization rate on the pore structure of PLGA scaffolds. (a) Depressurization rate of 3–6 MPa·min^{-1}; (b) depressurization rate of 0.3 MPa·min^{-1}; (c) depressurization rate of 0.1 MPa·min^{-1} (HA amount of 5%, soaking temperature of 55 °C, soaking pressure of 9 MPa).

CO_2 solubility in PLGA increased with the elevation of pressure, while the energy barrier for nucleation decreased exponentially [26,29]. Namely, more gas nuclei formed at the moment of depressurization, when more CO_2 was dissolved into PLGA at high soaking pressure. As a result, cellular scaffolds with a high density of pores could be fabricated at high soaking pressure, for example 15 MPa. However, bi-/multi-modal porous bone tissue engineering scaffolds could be fabricated at mild soaking pressure. In other words, low CO_2 solubility was available to prepare porous bone tissue engineering scaffolds in the process of $scCO_2$ foaming using HA as the heterogeneous agent.

3.3.3. The effect of depressurization rate on the pore structure of scaffolds

The effects of depressurization rate on PLGA scaffolds are shown in Figs. 3(d) and 6, and bimodal porous scaffolds were fabricated at 5% HA addition amount, soaking temperature of 55 °C and soaking pressure of 9 MPa with different depressurization rates. The size of small pores increased from (112 ± 29) μm to (230 ± 102) μm, and thickness of pore wall increased to (133 ± 82) μm with the decrease of depressurization rate from 3–6 MPa·min^{-1} to 0.1 MPa·min^{-1}; while the size of large pores didn't diminish evidently.

There are two competitions in $scCO_2$ foaming system as mentioned above. On the one hand, the degree of CO_2 supersaturation was decreased to nucleate less by slowing depressurization rate, thus more CO_2 diffused into nucleated pores to form large pores [17,28]. And at low depressurization rate, nucleated pores had enough time to merge and rupture to form bimodal porous structure with thick pore wall, which could enhance mechanical strength of scaffolds to some extent [26]. On the other hand, there were more CO_2 diffusing out of the polymer skin when the depressurization rate decreased. Besides, the decrease of temperature in autoclave and the vitrification of PLGA suppressed the growth of pores, especially at low depressurization rate [30]. In a whole, the pore structure and pore size of scaffolds were decided by the net effect of above factors.

3.4. The porosity and compression modulus of porous PLGA scaffolds

The porosity and compression modulus of prepared PLGA porous scaffolds under different depressurization rates are shown in Table 2.

Table 2
The porosity and compression modulus of porous PLGA scaffolds

Depressurization rate/MPa·min^{-1}	Porosity①/%	Porosity②/%	Compression modulus/MPa
3–6	94.48	82.30 ± 1.58	4.06 ± 0.98
1.5	96.55 ± 0.11	83.08 ± 2.42	2.67 ± 0.37
0.3	81.70	ND	12.96 ± 4.09
0.1	75.61	52.53 ± 2.69	18.15 ± 5.16

① Calculated from the density of PLGA before and after foaming.
② Measured by mercury intrusion porosimetry.

The total porosity calculated from the density of PLGA before and after foaming decreased from (96.55 ± 0.11% to 75.61)% with the decrease of depressurization rate to 0.1 MPa·min^{-1}, while the interconnected porosity measured by mercury intrusion porosimetry decreased from (83.08 ± 2.42)% to (52.53 ± 2.69)%. The compression modulus of scaffolds varied between (2.67 ± 0.37) and (18.15 ± 5.16) MPa.

Generally, low porosity facilitates osteogenesis by suppressing cell proliferation and forcing cell aggregation *in vitro*, while high porosity stimulates greater bone ingrowth *in vivo* [4]. Bone tissue engineering scaffolds with ideal properties should meet the requirements of porosity and mechanical property simultaneously, and the compression modulus of scaffolds fabricated in this work could satisfy the basic requirement of soft tissue (0.4–350 MPa) and hard tissue (10–1500 MPa) respectively at different depressurization rates [31].

4. Conclusions

Bi-/multi-modal porous PLGA/HA composite scaffolds used in bone tissue engineering were successfully prepared by supercritical CO_2 foaming. Specifically, HA particles were introduced as the heterogeneous nucleation agent, which would be helpful to cells proliferation and differentiation. Scaffolds with different pore structure could be obtained by controlling soaking temperature, pressure, depressurization rate and the addition amount of HA. The $scCO_2$ foaming was favorable to fabricate bone tissue engineering scaffolds due to the presence of HA particles, which facilitated the coalescence and rupture of pores to form bi-/multi-modal pore structure during the process of pore growth. Porosity and compression modulus of scaffolds fabricated by $scCO_2$ foaming could satisfy the basic requirement of bone tissue engineering scaffolds. Solvent-free $scCO_2$ foaming is a green method to prepare tissue engineering scaffolds, and thermal sensitive bioactive substances, *i.e.* proteins, can be incorporated into scaffolds by $scCO_2$ foaming under mild operation conditions.

References

[1] A.J. Salgado, O.P. Coutinho, R.L. Reis, Bone tissue engineering: State of the art and future trends, *Macromol. Biosci.* 4 (2004) 743–765.
[2] R. Langer, J. Vacanti, Tissue engineering, *Science* 260 (1993) 920–926.
[3] N. Harada, Y. Watanabe, K. Sato, S. Abe, K. Yamanaka, Y. Sakai, T. Kaneko, T. Matsushita, Bone regeneration in a massive rat femur defect through endochondral ossification achieved with chondrogenically differentiated MSCs in a degradable scaffold, *Biomaterials* 35 (2014) 7800–7810.
[4] V. Karageorgiou, D. Kaplan, Porosity of 3D biomaterial scaffolds and osteogenesis, *Biomaterials* 26 (2005) 5474–5491.
[5] A. Salerno, S. Zeppetelli, E. Di Maio, S. Iannace, P.A. Netti, Processing/structure/property relationship of multi-scaled PCL and PCL-HA composite scaffolds prepared via gas foaming and NaCl reverse templating, *Biotechnol. Bioeng.* 108 (2011) 963–976.
[6] H.Y. Mi, X. Jing, L.S. Turng, Fabrication of porous synthetic polymer scaffolds for tissue engineering, *J. Cell. Plast.* 51 (2014) 165–196.
[7] R.A. Quirk, R.M. France, K.M. Shakesheff, S.M. Howdle, Supercritical fluid technologies and tissue engineering scaffolds, *Curr. Opin. Solid State Mater. Sci.* 8 (2004) 313–321.

[8] D.J. Mooney, D.F. Baldwin, N.P. Suh, L.P. Vacanti, R. Langer, Novel approach to fabricate porous sponges of poly(D,L-lactic-co-glycolic acid) without the use of organic solvents, *Biomaterials* 17 (1996) 1417–1422.
[9] A. Salerno, S. Zeppetelli, E. Di Maio, S. Iannace, P.A. Netti, Architecture and properties of bi-modal porous scaffolds for bone regeneration prepared via supercritical CO_2 foaming and porogen leaching combined process, *J. Supercrit. Fluids* 67 (2012) 114–122.
[10] L.D. Harris, B.S. Kim, D.J. Mooney, Open pore biodegradable matrices formed with gas foaming, *J. Biomed. Mater. Res.* 42 (1998) 396–402.
[11] A. Salerno, S. Iannace, P.A. Netti, Graded biomimetic osteochondral scaffold prepared via CO_2 foaming and micronized NaCl leaching, *Mater. Lett.* 82 (2012) 137–140.
[12] X. Xin, Q.Q. Liu, C.X. Chen, Y.X. Guan, S.J. Yao, Fabrication of bimodal porous PLGA scaffolds by supercritical CO_2 foaming/particle leaching technique, *J. Appl. Polym. Sci.* 33 (2016) 43644.
[13] J. Colton, N. Suh, The nucleation of microcellular thermoplastic foam with additives. Part I: Theoretical considerations, *Polym. Eng. Sci.* 27 (1987) 485–492.
[14] J. Colton, N. Suh, The nucleation of microcellular thermoplastic foam with additives. Part II: Experimental results and discussion, *Polym. Eng. Sci.* 27 (1987) 493–499.
[15] J. Colton, N. Suh, Nucleation of microcellular foam theory and practice, *Polym. Eng. Sci.* 27 (1987) 500–503.
[16] I. Tsivintzelis, E. Pavlidou, C. Panayiotou, Biodegradable polymer foams prepared with supercritical CO_2–ethanol mixtures as blowing agents, *J. Supercrit. Fluids* 42 (2007) 265–272.
[17] L.M. Mathieu, T.L. Mueller, P.E. Bourban, D.P. Pioletti, R. Muller, J.A. Manson, Architecture and properties of anisotropic polymer composite scaffolds for bone tissue engineering, *Biomaterials* 27 (2006) 905–916.
[18] L. Mathieu, P. Bourban, J. Manson, Processing of homogeneous ceramic/polymer blends for bioresorbable composites, *Compos. Sci. Technol.* 66 (2006) 1606–1614.
[19] M. Salarian, W.Z. Xu, Z. Wang, T.K. Sham, P.A. Charpentier, Hydroxyapatite-TiO_2-based nanocomposites synthesized in supercritical CO_2 for bone tissue engineering: Physical and mechanical properties, *ACS Appl. Mater. Interfaces* 6 (2014) 16918–16931.
[20] A.M. Ng, K.K. Tan, M.Y. Phang, O. Aziyati, G.H. Tan, M.R. Isa, B.S. Aminuddin, M. Naseem, O. Fauziah, B.H. Ruszymah, Differential osteogenic activity of osteoprogenitor cells on HA and TCP/HA scaffold of tissue engineered bone, *J. Biomed. Mater. Res. A* 85 (2008) 301–312.
[21] M. Bhamidipati, A.M. Scurto, M.S. Detamore, The future of carbon dioxide for polymer processing in tissue engineering, *Tissue Eng. Part B Rev.* 19 (2013) 221–232.
[22] L.M. Mathieu, M.O. Montjovent, P.E. Bourban, D.P. Pioletti, J.A. Manson, Bioresorbable composites prepared by supercritical fluid foaming, *J. Biomed. Mater. Res. A* 75 (2005) 89–97.
[23] G.P. Chen, T. Ushida, T. Tateishi, A biodegradable hybrid sponge nested with collagen microsponges, *J. Biomed. Mater. Res.* 51 (2000) 273–279.
[24] N.S. Ramesh, Don H. Rasmussen, G.A. Campbell, The heterogeneous nucleation of microcellular foams assisted by the survival of microvoids in polymers containing low glass transition particles. Part I: Mathematical modeling and numerical simulation, *Polym. Eng. Sci.* 34 (1994) 1685–1697.
[25] N.S. Ramesh, Don H. Rasmussen, G.A. Campbell, The heterogeneous nucleation of microcellular foams assisted by the survival of microvoids in polymers containing low glass transition particles. Part II: Experimental results and discussion, *Polym. Eng. Sci.* 34 (1994) 1698–1706.
[26] I. Tsivintzelis, A.G. Angelopoulou, C. Panayiotou, Foaming of polymers with supercritical CO_2: An experimental and theoretical study, *Polymer* 48 (2007) 5928–5939.
[27] E. Reverchon, S. Cardea, Supercritical fluids in 3-D tissue engineering, *J. Supercrit. Fluids* 69 (2012) 97–107.
[28] H.Y. Tai, M.L. Mather, D. Howard, W.X. Wang, L.J. White, J.A. Crowe, S.P. Morgan, A. Chandra, D.J. Williams, S.M. Howdle, K.M. Shakesheff, Control of pore size and structure of tissue engineering scaffolds produced by supercritical fluid processing, *Eur. Cells Mater.* 14 (2007) 64–77.
[29] J.J. Barry, H.S. Gidda, C.A. Scotchford, S.M. Howdle, Porous methacrylate scaffolds: Supercritical fluid fabrication and in vitro chondrocyte responses, *Biomaterials* 25 (2004) 3559–3568.
[30] C. Marrazzo, E. Di Maio, S. Iannace, Conventional and nanometric nucleating agents in poly(ε-caprolactone) foaming: Crystals vs. bubbles nucleation, *Polym. Eng. Sci.* 48 (2008) 336–344.
[31] S.J. Hollister, Porous scaffold design for tissue engineering, *Nat. Mater.* 4 (2005) 518–524.